polaritons; in this case, the upper branch may be unstable (see the transition at $t \approx 700$ ps in Fig. 2). The cause of this second instability can be understood from Fig. 5c, d, showing the dispersion of eigenfrequencies of the linear problem in (6) and (7) in the absence of saturation calculated for the parameters $|\mathcal{P}_0|^2 = 0.44$ and $|\mathcal{E}_{\rm ext}|^2 = 0.083$, i.e., at the upper branch of the S-contour (see the star symbol on the solid curve in Fig. 4). As follows from Fig. 2, it is approximately this region into which the excited mode falls as a result of the development of the first instability at $t \approx 600$ ps. Then, the regions near $k_{\rm s} \approx 0$, $k_{\rm i} \approx 2k_{\rm p}$ (as shown in Fig. 5d) are characterized by very strong parametric instability with a large incremental growth. Unlike the figure eight during parametric scattering of polaritons on the lower branch of the S-contour [7, 32], the scattered signal on the upper branch of the S-contour reaches its maximum within compact solid angles inside the figure eight, close to $k_{\rm s} \approx 0$, $k_{\rm i} \approx 2k_{\rm p}$. This qualitatively agrees with experimental findings [13, 15]. Owing to the development of the second instability, the solution with a single macro-occupied mode decays: other polariton modes are rapidly populated (see also Fig. 3). As a result, the amplitude of the excited polariton abruptly decreases, and this state turns out to be more or less stable even if fluctuating in time because of rescattering on other polariton modes.

It must be noted in addition that taking the finiteness of saturation $V_{\rm sat} = 0.1$ into account leads to a quantitatively different position of the S-curve (cf the solid and dashed curves in Fig. 4) but does not cause a qualitative change in the scattering scenario. This follows, for example, from the smallness of the difference between the eigenfrequencies of the linear problem (6), (7) for $V_{\rm sat} = 0$ and $V_{\rm sat} = 0.1$ calculated at characteristic jump points on the corresponding S-curve (see Fig. 6).

To summarize, using a simplified quasi-one-dimensional model of polariton – polariton scattering in MCs, we have numerically demonstrated the feasibility of a hard-threshold stimulation of polariton – polariton scattering while smoothly varying the external pump. This is possible due to the mutual influence of bistability of the response of the excited polariton mode and its instability relative to parametric pump. The resultant scattered signal proves to be directed roughly normally to the microcavity, $k_{\rm s} \approx 0$, in qualitative agreement with experiment [13, 15]. The analysis of stability of polariton – polariton scattering indicates that this result must be preserved when taking the quasi-two-dimensionality of the scattering and excitonic saturation into account. In conclusion, we emphasize that an essential condition for the existence of an instability region on the upper branch of the S-shaped curve of a nonlinear oscillator with respect to the scattering into other polariton modes is the presence of an inflection point at the lower polariton dispersion branch. In the case of an empty MC with a quadratic dispersion or pump far away from the inflection region, there is no such instability, and the behavior of the system proves simply bistable.

The authors are grateful to P V Elyutin and N S Maslova for helpful discussions. The work was supported in part by the RFBR and INTAS.

References

1. Savvidis P G et al. *Phys. Rev. Lett.* **84** 1547 (2000)
2. Houdré R et al. *Phys. Rev. Lett.* **85** 2793 (2000)
3. Ciuti C et al. *Phys. Rev. B* **62** R4825 (2000)
4. Tartakovskii A I, Krizhanovskii D N, Kulakovskii V D *Phys. Rev. B* **62** R13298 (2000)
5. Stevenson R M et al. *Phys. Rev. Lett.* **85** 3680 (2000)
6. Baumberg J J et al. *Phys. Rev. B* **62** R16247 (2000)
7. Ciuti C, Schwendimann P, Quattropani A *Phys. Rev. B* **63** 041303 (2001)
8. Whittaker D M *Phys. Rev. B* **63** 193305 (2001)
9. Savvidis P G et al. *Phys. Rev. B* **64** 075311 (2001)
10. Saba M et al. *Nature* **414** 731 (2001)
11. Savasta S, Di Stefano O, Girlanda R *Phys. Rev. Lett.* **90** 096403 (2003)
12. Huynh A et al. *Phys. Rev. Lett.* **90** 106401 (2003)
13. Kulakovskii V D et al. *Nanotechnology* **12** 475 (2001)
14. Kulakovskiĭ V D et al. *Usp. Fiz. Nauk* **175** 334 (2005) [*Phys. Usp.* **48** 312 (2005)]
15. Butté R et al. *Phys. Rev. B* **68** 115325 (2003)
16. Gippius N A et al., in *Proc. of the 26th Intern. Conf. on the Physics of Semiconductors, Edinburgh, UK, 29 July – 2 August 2002* (Institute of Physics Conf. Ser., No. 171, Eds A R Long, J H Davies) (Bristol: IOP Publ., 2003) p. G4-6
17. Kulakovskiĭ V D et al. *Usp. Fiz. Nauk* **173** 995 (2003) [*Phys. Usp* **46** 967 (2003)]
18. Gippius N A et al. *Europhys. Lett.* **67** 997 (2004)
19. Gippius N A, Tikhodeev S G *J. Phys.: Condens. Matter* **16** S3653 (2004)
20. Baas A et al. *Phys. Rev. A* **69** 023809 (2004)
21. Whittaker D M, in *Proc. of PLCMN4, St. Petersburg, June 2004* (2004)
22. Carusotto I, Ciuti C *Phys. Rev. Lett.* **93** 166401 (2004)
23. Tikhodeev S G et al. *Phys. Rev. B* **66** 045102 (2002)
24. Tassone F, Yamamoto Y *Phys. Rev. B* **59** 10830 (1999)
25. Firth W J, Scroggie A J *Phys. Rev. Lett.* **76** 1623 (1996)
26. Kuszelewicz R et al. *Phys. Rev. Lett.* **84** 6006 (2000)
27. Vladimirov A G et al. *Phys. Rev. E* **65** 046606 (2002)
28. Duffing G *Erzwungene Schwingungen bei veränderlicher Eigenfrequenz* (Braunschweig: Vieweg, 1918)
29. Luchinsky D G, McClintock P V E, Dykman M I *Rep. Prog. Phys.* **61** 889 (1998)
30. Gilmore R *Rev. Mod. Phys.* **70** 1455 (1998)
31. Baas A et al. *Phys. Rev. B* **70** 161307(R) (2004)
32. Langbein W *Phys. Rev. B* **70** 205301 (2004)

PACS numbers: **42.65.–k**, **71.36.+c**, **78.65.–n**
DOI: 10.1070/PU2005v048n03ABEH002126

Stimulated polariton – polariton scattering in semiconductor microcavities

V D Kulakovskii, D N Krizhanovskii,
M N Makhonin, A A Demenev,
N A Gippius, S G Tikhodeev

Mixed exciton – photon states in planar semiconductor microcavities (MCs) with quantum wells (QWs) in a $1-3\,\lambda$ thick active layer (where λ is the wavelength of light) represent a new class of quasi-two-dimensional particles having unique properties [1]. Such states, called microcavity polaritons, are realized in MCs if the decay of both the photon and exciton modes does not exceed the exciton – photon interaction energy. Light quantization in a planar MC perpendicular to the plane of the mirrors leads to an almost parabolic dispersion of the photon mode with a very small effective mass near zero lateral quasi-momentum **k**,

$$E_{\rm C} = \left(E_{\rm C}^2(0) + \frac{(\hbar c k)^2}{\varepsilon} \right)^{1/2}, \qquad (1)$$

where $\hbar$ is the Planck constant, c is the speed of light, and ε is the dielectric constant. In the strong exciton–photon coupling regime, the exciton and photon modes undergo mutual repulsion giving rise to two — upper and lower — polariton branches, whose dispersion is determined by two parameters, the energy detuning $\delta = E_C - E_X$ between the empty MC photon mode (E_C) and the exciton (E_X) at point $\mathbf{k} = 0$ and the exciton–photon coupling Ω. Because the photon component contribution is large, the effective mass of MC-polaritons turns out to be several orders of magnitude smaller than that of excitons, while their coherence length reaches several microns. These two factors account for a qualitative change in the properties of the excitonic system [1–3]. Unique polariton dispersion in MCs, on the one hand, and the short polariton lifetime, on the other hand, are responsible for the polariton energy relaxation in MC-structures being significantly different from exciton relaxation in QWs.

The strong k-dependence of the MC-polariton energy at small k leads, in a similar manner to three-dimensional polaritons in semiconductors, to the marked suppression of the acoustic-phonon-assisted energy relaxation. Hence, a markedly decreased population of the states close to the bottom of the lower polariton branch (LPB) at small excitation densities is observed, called the 'bottleneck effect' [4]. With the strongly suppressed polariton–phonon relaxation mechanism, the interparticle scattering acquires importance [5, 6]. In particular, polariton scattering on electrons even at a small density of the two-dimensional electron gas in QWs results in a stronger energy relaxation of polaritons compared with their scattering on phonons. This leads to the strong dependence of the polariton energy distribution in the LPB under photoexcitation conditions [7–9].

Researchers have recently given much attention to polariton–polariton scattering, due to which the exciton–polariton system exhibits strong nonlinear properties manifested in the behavior of radiation intensity and polarization at large resonant excitation densities close to the inflection point of the LPB dispersion curve [2, 3, 10–17]. Specifically, such excitation results in the appearance of strong parametric scattering into states with $\mathbf{k} = 0$ and $2\mathbf{k}_p$, where $\mathbf{k}_p$ is the quasi-momentum of the exciting light. This effect can be explained by the four-wave mixing (FWM) or parametric scattering of photoexcited polaritons out of the state $(E_p, \mathbf{k}_p)$ with the energy E_p and momentum $\mathbf{k}_p$ to states $(E_s, \mathbf{k}_s)$ and $(E_i, \mathbf{k}_i)$, called the 'signal' (S) and the 'idler' (I) states, respectively. The effect occurs with the energy and quasi-momentum being conserved,

$$\mathbf{k}_s + \mathbf{k}_i = 2\mathbf{k}_p\,, \qquad E_s + E_i = 2E_p\,. \tag{2}$$

The conversion coefficient being as large as 10%, MC-structures appear very promising for application in thresholdless polariton lasers [18].

Initially, the observed effects were described in terms of the FWM model [2, 10–13] developed for the description of a system with a single macro-occupied mode $E_p, \mathbf{k}_p$. Indeed, for excitation at the inflection point of the LPB, the laws of energy and momentum conservation (2) are satisfied for $\mathbf{k}_s = 0$ and $\mathbf{k}_i = 2\mathbf{k}_p$. But subsequent studies have demonstrated that at pump intensities above a certain critical value, even if the excitation occurs rather far from the inflection point, the scattering is into states $\mathbf{k}_s = 0$ and $\mathbf{k}_i = 2\mathbf{k}_p$, as before. The energy conservation is then satisfied because E_s and E_i lie much above the polariton branch. Potential causes of such behavior are discussed in Refs [19–23]. In particular, it was found that the hard polariton–polariton scattering regime can be realized at high polariton excitation densities close to the inflection point due to the overlap between the regions of polariton instability with respect to the polariton–polariton decay and polariton bistability typical of a nonlinear oscillator. It is worth noting that bistability of the linear response of MCs in the LPB minimum region was recently studied both experimentally and theoretically in Ref. [24]. Moreover, it was theoretically shown [25] that bistability of the response of nonlinear polaritons may lead to their superfluidity.

The present paper is concerned with experimental aspects of the problem under consideration with special reference to the results of the polariton–polariton scattering studies in a GaAs-based semiconductor MC-structure (Fig. 1). This structure consists of two Bragg reflectors, with the front one composed of 17 and the rear one of 20 repetitive $Al_{0.13}Ga_{0.87}As/AlAs$ layers ($\lambda/4$), and the active layer with InGaAs quantum wells. The structure was grown by molecular-beam epitaxy on a 0.5 mm thick GaAs substrate. The MC active layer composed of GaAs and having the thickness $3/2\lambda$ contained six 10 nm thick $In_{0.06}Ga_{0.94}As/GaAs$-quantum wells. The Rabi splitting $\Omega \sim 6$ meV. The microcavity was grown such that the thickness of its active layer gradually varied along the sample length leading to a change in the photon mode energy E_C and, accordingly, in a mismatch between the exciton energy E_X and the photon mode energy in states with $k = 0$. The experiments were designed to investigate sample regions with the δ value from -2 to $+1$ meV.

Two solid-state continuous Ti–Sp lasers were used for resonant photoexcitation of polaritons. The nonresonant excitation above the band gap was performed with an He–Ne laser. The specimen was placed in a liquid helium cryostat where the temperature was varied in the range from 5 to 15 K by a thermoregulation system accurate to within 0.05 K. Photoluminescence (PL) was collected at various angles using lenses and an optical fibre, all mounted on a goniometer arm. Angular resolution was achieved by a diaphragm controlling a solid angle of 0.5°. The PL signals were recorded with a 1-m double monochromator and a nitrogen-cooled CCD detector.

High angular resolution spectroscopy makes it possible to resonantly excite polaritons with a given quasi-momentum and to measure the polariton distribution in momentum space by independently choosing the photoexcitation and observation angles. The tangential component of the light momentum at the vacuum–MC boundary being conserved, the polariton quasi-momentum $|\mathbf{k}|$ and the incidence angle Φ are related by the simple expression $k = |\mathbf{k}| = (E/c)\sin\Phi$. Because the experiments were carried out under continuous excitation conditions, both the momentum and the energy of polaritons were determined with high accuracy.

Figure 1 shows MC emission spectra for the LPB excited resonantly by σ^+-polarized light at the inflection point. For weak excitation, both the intensity and the polarization degree of the emission line decrease with the approach to the bottom of the LPB band, the transition energies being the same for σ^+- and σ^--polarizations. Such behavior is consistent with the expected one for polaritons with a strong 'bottleneck effect' for their energy relaxation. A rise in the excitation density brings no change in the σ^--spectra, whereas the σ^+-polarized emission line near $k = 0$ narrows consider-

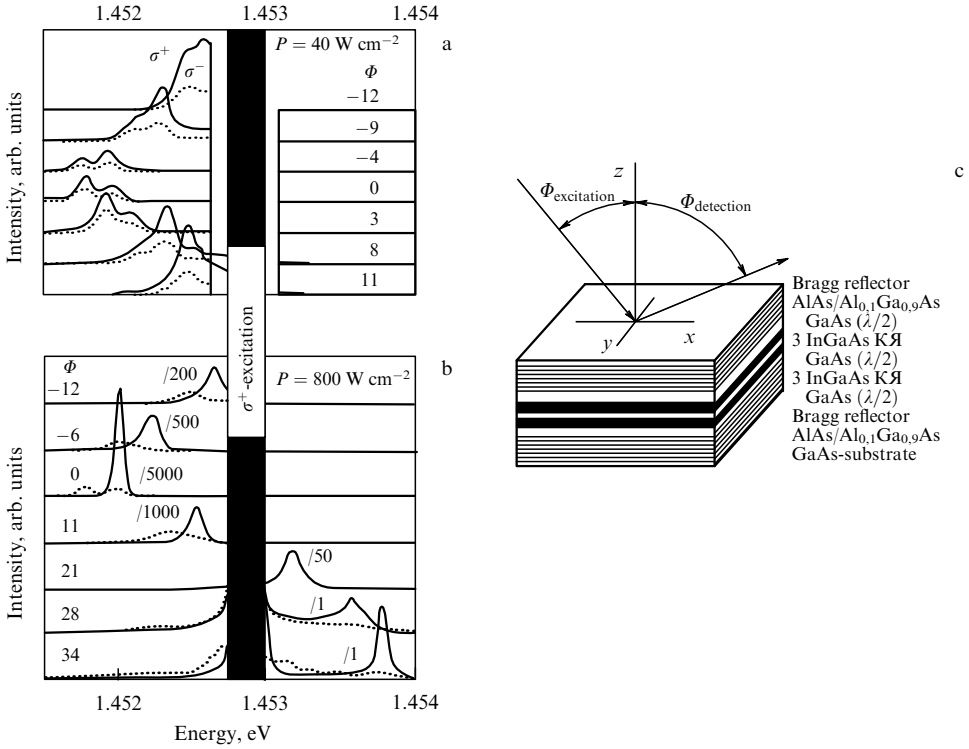

Figure 1. Angular dependences of the MC emission spectra at weak (a) and strong (b) resonant σ^+-photoexcitation recorded for two polarizations; values of the angle Φ are given in degrees; the black vertical strip corresponds to the pump line where the photoluminescence signal was not measured. (c) Schematic representation of the studied microcavity containing QWs in the active layer.

ably and shifts to the blue region, while its intensity grows exponentially with the excitation density. As a result, the emission becomes almost 100% σ^+-polarized at high excitation densities. Simultaneously, the idler emerges at the quasi-momentum $\mathbf{k} = 2\mathbf{k}_p$ above the excitation energy, in accordance with Eqn (2). The appearance of line I in the spectrum indicates that parametric scattering actually makes an important contribution, and the threshold growth of the signal suggests the self-stimulating nature of the scattering. Such a regime is realized when the occupation of states near $k = 0$ exceeds unity and results in additional stimulation of scattering into these states by virtue of the bosonic nature of polaritons.

The signal behavior at large excitation densities in a region with $k \sim 0$ at a fixed excitation angle strongly depends on whether the exciting quantum energy E_p shifts to above or below the polariton branch. If E_p shifts below the LPB, the threshold for stimulated scattering sharply increases to exceed 1,000 W cm^{-2} even at a detuning as small as -0.05 meV. As the laser frequency increases above the LPB, the threshold power for stimulated scattering P_{th} grows much more slowly. Simultaneously, in conflict with the simple four-wave mixing theory, the values of $\mathbf{k}_s$ and $\mathbf{k}_i$ remain virtually unaltered at all E_p, while lines S and I shift to energies well above the LPB. This situation is illustrated by Fig. 2, showing the distribution of the emission intensities upon excitation to 0.1 and 1 meV above the LPB (E_{LP}). It follows from Fig. 2 that at the excitation 1 meV above the LPB, both E_S and E_I move approximately 1 meV above the LPB, in agreement with the energy conservation law.

Theoretical studies [19, 20] were designed to simulate the process of parametric scattering of MC-polaritons based on a system of two coupled equations, the Maxwell equation and an inhomogeneous nonlinear Schrödinger equation for exciton polarization that includes two types of sources, a coherent external excitation and a stochastic Langevin noise. To simplify computation, a one-dimensional problem was solved and mixing of σ^+ and σ^--polarizations in the Maxwell equation was neglected (in other words, it was written in the resonant scalar approximation). As a result, the equations for the QW electric field E_{QW} and the QW-width-averaged exciton polarization $P(k,t)$ assumed the form

$$\begin{aligned}
&\left[\mathrm{i}\,\frac{\mathrm{d}}{\mathrm{d}t} - E_C(k)\right]\mathcal{E}_{QW}(k,t) = \alpha(k)\,\mathcal{E}_{ext}(k,t) + \beta(k)\,P(k,t)\,,\\
&\left[\mathrm{i}\,\frac{\mathrm{d}}{\mathrm{d}t} - E_X(k)\right]P(k,t)\\
&\quad = F\sum_{q,q'} P(q,t)\,P^*(q+q'-k,t)\,P(q',t)\\
&\quad + A\mathcal{E}_{QW}(k,t) + \xi(k,t)\,.
\end{aligned} \tag{3}$$

Here, $\mathcal{E}_{ext}(k,t) = \mathcal{E}(t)\exp(-\mathrm{i}\omega_p t)\,\delta(k-k_p)$ is the electric field of the incident electromagnetic pump wave far from the MC, E_C and E_X are the respective resonance mode energies of the empty MC and the exciton in the QW, F is the exciton–exciton coupling constant, A is the exciton polarizability, and $\xi(k,t)$ is the Langevin random force,

$$\langle\xi(k,t)\rangle = 0\,,\quad \langle\xi(k,t)\,\xi(k',t')\rangle \propto \delta(k-k')\,\delta(t-t')\,.$$

The MC response constants α and β were calculated using the scattering matrices. In the calculations, the electric field of the exciting wave was fixed instead of the QW field and all paired polariton–polariton collisions were taken into account.

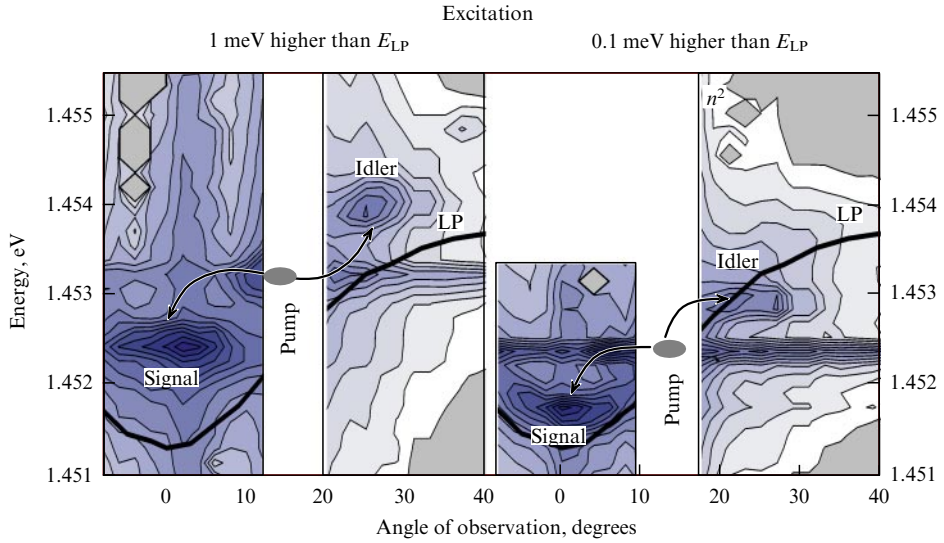

Figure 2. Distribution of the emission intensity upon excitation with the power density 1300 W cm^{-2} at the angle corresponding to the inflection point of the LPB curve by a laser with the quantum energy 0.1, 1 meV above the LPB. The dark areas correspond to higher emission intensities.

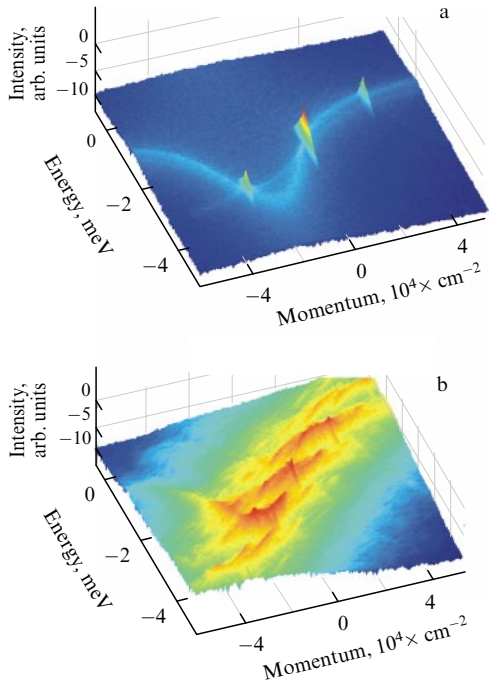

Figure 3. Calculated angular distribution of the polariton emission intensity upon excitation of the LPB to 0.3 meV above E_C for two excitation densities, 3% lower (a) and 3% higher (b) than the critical value for the development of the stimulated parametric scattering regime [20]. The energy is counted from $E_C(k=0)$. The relative intensity of scattered polaritons (normalized to the pump intensity) is plotted along the vertical line in a logarithmic scale.

Figure 3 presents the calculated angular distribution of the emission intensity at the excitation densities 3% lower and 3% higher than the critical value for the development of the stimulated parametric scattering regime.

It can be seen from Fig. 3 that at $P < P_{th}$, the standard four-wave mixing regime with the signal and idler modes lying on the dispersion curve is realized, with the quasi-momentum of the signal mode differing from zero. But as P_{th} is exceeded only by 3%, the angular distribution pattern of the emission intensity is drastically altered. The signal grows by several orders of magnitude and the scattering maximum shifts to the region with $k \sim 0$ and is qualitatively consistent with the experimental one (see Fig. 2). Thus, the comparison of the experimental and theoretical findings indicates that the model for the description of stimulated scattering of excitonic polaritons in a semiconductor MC proposed in Refs [20–22] may be used to qualitatively describe the experimental results. However, it does not explain some details of the development of stimulated scattering. In particular, it is assumed in the calculation that the difference between the behavior of polariton–polariton scattering in an MC and that predicted by the standard FWM model is attributable to the competition of two instabilities. At the initial stage, the amplitude of the excited polariton mode undergoes a jump due to the development of its instability characteristic of a nonlinear oscillator. As a result of the concurrent transformation of the pump mode, the system passes to the region of another instability, i.e., the instability with respect to polariton–polariton scattering into other modes. The appearance of this region is due to the specific dispersion of the LPB with an inflection point. This instability is responsible for the threshold build-up of filled polariton modes in a large phase-space domain while the scattered signal becomes strongly stochastic. Concurrently, the parametric scattering to the most densely occupied modes near $k \sim 0$ becomes dominant. Although the system is assumed to be spatially uniform in Refs [20–22], it can be expected to break down into spatially inhomogeneous regions.

Polarization in quantum wells of MCs can be experimentally assessed by the FWM technique in which an additional test laser with energy E_t is employed as shown in Fig. 4a. The intensity of a FWM signal is given by

$$I_{FWM}(E_{FWM} = 2E_p - E_t) \sim f(E_{FWM})\, P_t \left|\mathcal{E}_{QW}(E_p)\right|^4, \quad (4)$$

where P_t is the power density of the test laser and the factor $f(E_{FWM})$ reflects a change in the cavity transmittance with varying E_{FWM}; in fact, it monotonically decreases with the distance of E_{FWM} from $E_{LP}(2\mathbf{k}_p)$.

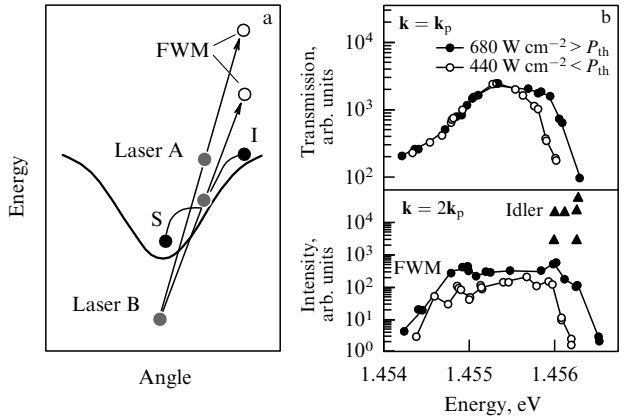

Figure 4. (a) Schematic for measuring the electric field in a QW by FWM with the use of two lasers; the frequency of the test pump laser B is below $E_p(\mathbf{k} = 0)$, the frequency of the pump laser A varies in the vicinity of the polariton branch energy at $\mathbf{k} = \mathbf{k}_p$ close to the inflection point of the LPB dispersion curve; the signal is measured at the quasi-momentum $\mathbf{k} = 2\mathbf{k}_p$ simultaneously with the idler of stimulated parametric scattering. (b) Transmission spectra at $\mathbf{k} = \mathbf{k}_p$ (top) and spectral dependences of the intensity $I_{FWM}(E_p)$ on the quasi-momentum $\mathbf{k} = 2\mathbf{k}_p$ (bottom) in the case of frequency variation of the pump laser A in the resonance region with a polariton mode for excitation densities above and below P_{th}.

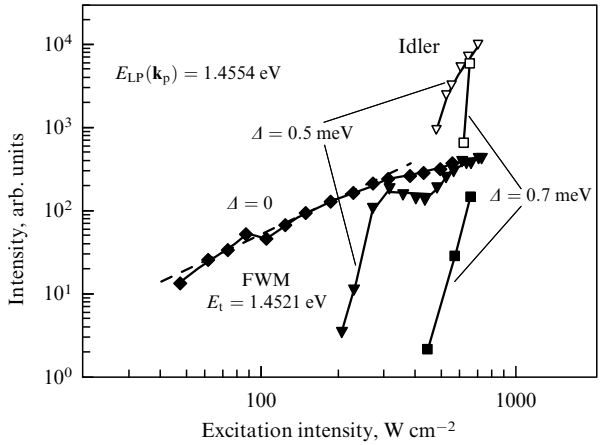

Figure 5. Dependences of the $E_p - E_t$ FWM signal (dark symbols) and the idler of parametric scattering (white symbols) on the excitation density P_p for various detunings Δ between the pump laser frequency E_p and the LPB frequency at the pump angle $E_{LP}(\mathbf{k}_p)$.

Figure 4b presents spectral dependences of the FWM written at the pump pulse $k_p = 1.6$ cm^{-1} fixed close to the inflection point of the LPB curve and variation of the pump laser frequency E_p near $E_{LP}(\mathbf{k}_p)$. For the test laser B, we chose $k_t = 0$ and the energy $E_t = 1.4521$ eV $< E_{LP}(k = 0)$. In this case, the signal of the FWM is observed at $\mathbf{k}_{FWM} = 2\mathbf{k}_p$ and lies above the LPB at $\mathbf{k} = 2\mathbf{k}_p$. Owing to the choice of $k_t = 0$, the spectrum written at $\mathbf{k} = 2\mathbf{k}_p$ contains both the signal I_{FWM} from the mixed waves E_p and E_t and the idler I from the stimulated parametric scattering. Measurements of the dependence of I_{FWM} on the test laser power density confirmed that at a fixed P_p, the intensity $I_{FWM} \sim P_t$ in a broad range $P_t < 300$ W cm^{-2}.

A change in the intensity $I_{FWM}(E_p)$ at the quasi-momentum $\mathbf{k} = 2\mathbf{k}_p$ upon variation of the frequency of the pump laser A in the resonance region with a polariton mode is shown in Fig. 4b, along with the transmission of laser radiation at $\mathbf{k} = 2\mathbf{k}_p$ for two excitation densities (above and below P_{th}). The dependence $I_{FWM}(E_p)$ measured at a fixed excitation density reflects, to within the factor f changing relatively weakly with frequency, the frequency dependence of the electric field in a QW at a given external field. Comparison of the transmission and four-wave mixing signals in Fig. 4b indicates that $I_{FWM}(E_p)$ coincides with the position of the polariton mode (the small redshift is related to the enhanced cavity transmittance as E_{FWM} approaches E_{LP}). With a rise in the excitation density $P(E_p)$ from 440 to 680 W cm^{-2}, $I_{FWM}(E_p)$ somewhat broadens and the maximum value increases less than two-fold. The spectral dependence I_{FWM} is qualitatively different from the spectral dependence of the stimulated parametric scattering signal also depicted in Fig. 4b. This signal emerges in a threshold manner at $P(E_p) > 450$ W cm^{-2} and can be seen at 680 W cm^{-2} in a very thin spectral region at the blue end of the line I_{FWM}.

The dependences of the intensity $I_{FWM}(P_p)$ at different detunings $\Delta = E_p - E_{LP}(\mathbf{k}_p)$ ($E_{LP} = 1.4554$ eV) and at the blue edge in the region of the observable stimulated parametric scattering signal 1.45602 – 1.45626 eV are presented in Fig. 5. In the absence of a detuning ($\Delta = 0$, black rhombi), there is no instability of the response of a nonlinear oscillator at the pump angle, i.e., the intensity $I_{FWM} \sim P_p^2$ in the region of small excitations $P_p < 150$ W cm^{-2} and assumes a subquadratic dependence as P_p continues to increase. In the case of a positive detuning ($\Delta = 0.5$ and 0.7 meV), stimulated parametric scattering occurs (open squares and triangles). The dependence $I_{FWM}(P_p)$ (black squares and triangles) manifests a threshold nature suggesting the passage through the bistable behavior region. The FWM signal begins to be recorded against the background of a weak luminescence signal at a certain critical excitation density P_{cr}. When the value of P_{cr} is exceeded by only 1.5-fold, I_{FWM} increases by more than two orders of magnitude, exhibiting a threshold behavior. As expected, the boundary value P_{cr} for the threshold growth of I_{FWM} rapidly increases with increasing Δ. It follows from Fig. 5 that at $\Delta = 0.5$ meV, I_{FWM} assumes a subquadratic dependence on P_p at higher excitation densities than at $\Delta = 0$. Such dependence of the intensity $I_{FWM}(P_p)$ suggests an instability of the response of the polartion oscillator at the frequencies at which stimulated parametric scattering occurs. This observation is consistent with the predictions in Refs [19, 20]. However, two important experimental findings should be taken into consideration. Specifically, the stimulated parametric scattering at $\Delta = 0.7$ meV starts to develop immediately after the passage of the polariton oscillator onto the upper branch of the S-shaped curve of the nonlinear oscillator. Conversely, at $\Delta = 0.5$ meV, the QW electric field that passed onto the upper branch remains too small for the instability with respect to polariton – polariton scattering to develop. The instability arises no sooner than the excitation density amounts to 500 W cm^{-2}, while the electric field in the QW increases by only 15%.

The threshold growth of the idler peak in the region of a virtually constant field in a QW indicates that it is associated with the macro-occupation of polariton states at the bottom of the LPB. The population of these states may be due not only to the direct polariton – polariton scattering but also to the phonon and electron assisted polariton scattering. We studied temperature dependences of parametric scattering in

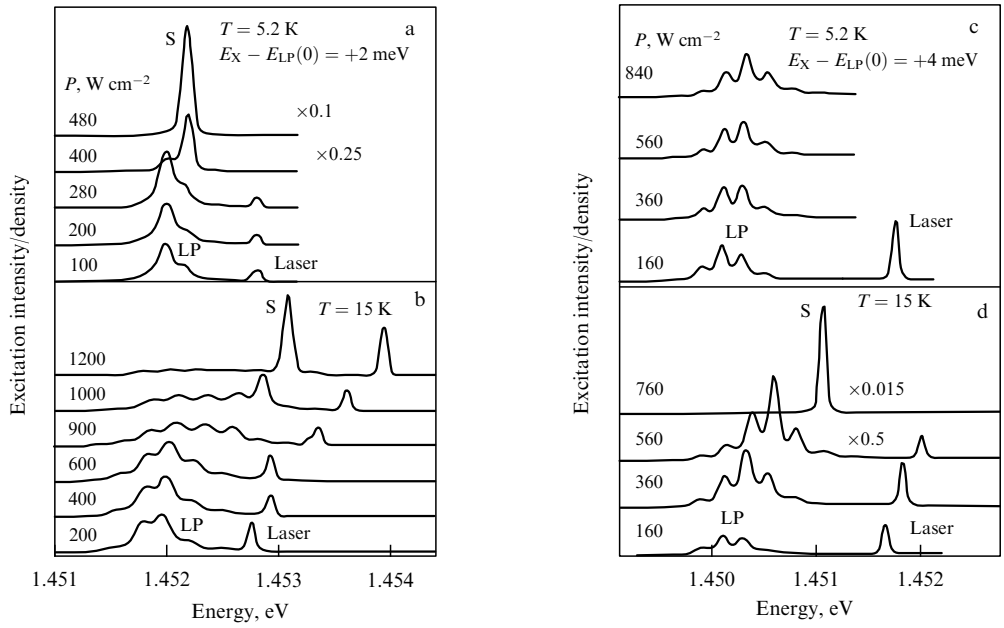

Figure 6. MC emission spectra at different excitation densities near the inflection point of the LP-branch ($k_p = 1.9 \times 10^4$ cm^{-1}) for two points on the sample corresponding to the LPB depths $E_X - E_{LP}(0) = 2$ meV (a, b) and 4 meV (c, d) at $T = 5.2$ and 15 K. In recording the emission spectra, the laser frequency was slightly adjusted in order to obtain a maximum signal.

MCs with different depths of the polartion branch in order to assess the role of additional polariton scattering mechanisms in the formation of stimulated parametric scattering.

Figure 6 depicts MC emission spectra in the case of excitation close to the inflection point of the LP-branch ($k_p = 1.9 \times 10^4$ cm^{-1}) for two points on the sample corresponding to the LPB depths $E_X - E_{LP} = 2$ and 4 meV, at $T = 5$ and 15 K. In recording the emission spectra, the laser frequency was slightly adjusted in order to obtain a maximum signal. The shift $\Delta = E_p - E_{LP}(k_p)$ was absent at small excitation densities but increased with growing P_p to amount to 0.2 meV at $T = 5$ K and ~ 1 meV at $T = 15$ K. The fine peak structure at a small excitation density is attributable to interference on the front and rear sides of the sample.

It can be seen from Fig. 6 that in an MC with a small depth of the polariton mode, the stimulated scattering threshold grows with rising the temperature. Such behavior is not unexpected because, as the temperature rises, polariton scattering by phonons and thermally excited excitons (and especially electrons) must lead to the enhancement of polariton scattering out of the macro-occupied signal and idler modes. Also expected is the growth of P_{th} with increasing the depth of the polariton branch observed at $T = 5$ K. Indeed, the deeper the polariton mode, the smaller the exciton component in the polariton, while its damping becomes faster because the damping of the MC-mode in the MC under study with a quality factor of 3000 is roughly one order of magnitude greater than that of the excitons.

At the same time, the temperature behavior of the stimulated scattering threshold in MC having a deep LPB is a great surprise. It can be seen from Fig. 6 that P_{th} in an MC with the LPB depth 4 meV decreases almost two-fold as the temperature increases from 5 to 15 K. Moreover, the comparison of Figs 6b and 6d shows that at 15 K, P_{th} grows with decreasing the LPB depth, even though the damping of the polariton mode slows down. Evidently, both the decrease in P_{th} with increasing the temperature in the deep LPB and the decrease in P_{th} with deepening the LPB at elevated temperatures are in contradiction with the predictions of the standard FWM theory. Besides, these experimental data indicate that the model of polariton parametric scattering in MCs proposed in Refs [19–22] is insufficient to account for the stimulated parametric scattering of MC polaritons. Specifically, these data indicate that the stimulated parametric scattering may be due not only to polariton instability with respect to the parametric scattering attributable to the specific dispersion of the polariton branch but also to noncoherent processes of polariton scattering on phonons, hot excitons, and free carriers. The increasing importance of noncoherent processes with the deepening of the polariton branch is associated with the suppression of the thermal excitation of polaritons from the bottom of an LPB having a depth in excess of kT.

The effect of noncoherent polariton scattering from free electrons on the stimulation of parametric scattering can also be traced in experiments on parametric scattering at the resonant excitation near the inflection point of an LPB with an additional above-gap excitation of free carriers using an He–Ne laser. Indeed, as shown in Refs [7, 9], the hot photoexcited carriers markedly accelerate the polariton ralaxation to the bottom of the polariton branch in an MC with a deep LPB at low temperatures.

Figure 7 illustrates the effect of a weak (40 W cm^{-2}) additional excitation of hot excitons and free carriers at the stimulated parametric scattering threshold under excitation of an LPB close to the inflection point at $T = 5.2$ K. The threshold of stimulated parametric scattering in this sample excited by a Ti–Sp laser alone is reached at 1200 W cm^{-2}. The emission intensity under the above-gap excitation by a He–Ne laser with a power density of 40 W cm^{-2} is similar to that under weak (around 30 W cm^{-2}) resonant excitation. However, the figure shows that simultaneous excitation by two lasers results in stimulated parametric scattering at $P_{Ti-Sp} = 840$ W cm^{-2}. In other words, a relatively small

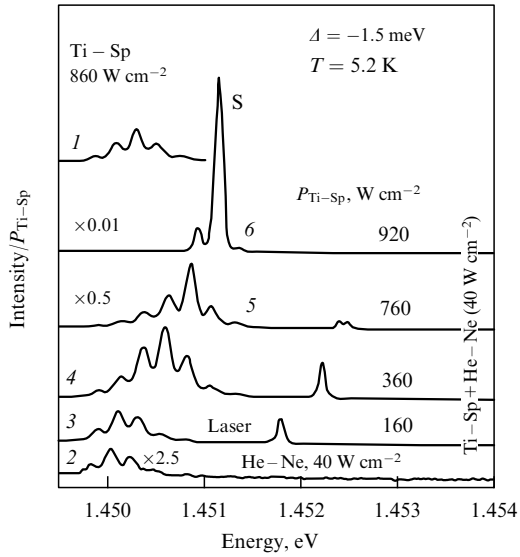

Figure 7. Polariton emission spectra in an MC with $E_X - E_{LP}(0) \sim 4.5$ meV $= 53$ K at $T = 5.2$ K and different excitation densities: resonant excitation by a Ti – Sp laser alone with the density 860 W cm^{-2} (curve *1*), weak excitation (40 W cm^{-2}) above the band gap by an He – Ne laser alone (curve *2*), and combined excitation by the two lasers (curves *3 – 6*) with a fixed excitation density of the He – Ne laser (40 W cm^{-2}) and varying resonant excitation density of the Ti – Sp laser (indicated by figures above the curves).

nonequilibrium concentration of photoexcited hot excitons and electrons (10^9 cm^{-2}) lowers the parametric scattering threshold by a factor of 1.5. Comparison of the behavior of P_{th} under temperature variations and an additional above-band-gap excitation indicates that the effect of photoexcited hot excitons and carriers on P_{th} is similar to the effect of phonons at an elevated temperature.

The lowering of the stimulated parametric scattering threshold with increasing the temperature or adding hot electrons to the polariton system can be accounted for by the fact that polariton – photon and polariton – electron collisions result in the enhanced population of the polariton states at the bottom of the LPB. The polariton state density at the bottom of the LPB being rather low (approximately four orders of magnitude lower than for excitons), their filling can be controlled by relatively small changes in the rate of noncoherent relaxation of polaritons caused by polariton – phonon and polariton – electron collisions.

To summarize, investigations into stimulated parametric scattering of excitonic polaritons in planar MCs have demonstrated that this scattering cannot be described in the framework of the standard FWM model with a single macro-occupied mode. Theoretical studies [19, 20] have qualitatively reproduced the experimentally observed effect, i.e., the marked rearrangement of the spectrum of the scattered polaritons resulting in the appearance of maxima at $k \sim 0$ and $\mathbf{k} \sim 2\mathbf{k}_p$ and followed by an increase by several orders of magnitude in the total scattered signal intensity, instead of parametric swinging of the macro-occupied modes at $k \neq 0$ and $\mathbf{k} \neq 2\mathbf{k}_p$. The physical mechanism of this transition is related to the parametric instability of the decay of a pump polariton into S- and I-polaritons above a certain critical pump intensity. Also, it is related to the presence of an absolutely unstable negative-slope region on the S-shaped plot showing the way the exciton polarization on the quasi-momentum of the exciting laser beam varies with the pump amplitude [19 – 23]. It is worthwhile noting that such an S-shaped dependence leads, for example, to the recently discovered bistability of the linear response in the LPB minimum region [24]. However, the proposed model is still unfit to quantitatively describe the experimental findings. Specifically, it does not cover polariton – phonon and polariton – electron interactions. Therefore, it does not explain the experimentally observed unusual behavior of the stimulated scattering threshold, i.e., its lowering with a temperature rise in the MC with a relatively deep LPB and in the case of the injection of very small quantities of free electrons. The description of these phenomena requires the consideration of the process of noncoherent polariton scattering on phonons and free carriers at the bottom of the LPB.

The authors are grateful to L V Keldysh, A I Tartakovskii, and V B Timofeev for numerous discussions and M Skolnick for providing the samples and helpful discussions. The work was supported in part by the Russian Foundation for Basic Research and INTAS.

References

1. Weisbuch C et al. *Phys. Rev. Lett.* **69** 3314 (1992)
2. Baumberg J J et al. *Phys. Rev. B* **62** R16247 (2000)
3. Kulakovskiĭ V D et al. *Usp. Fiz. Nauk* **173** 995 (2003) [*Phys. Usp.* **46** 967 (2003)]
4. Tassone F et al. *Phys. Rev. B* **56** 7554 (1997)
5. Tartakovskii A I et al. *Phys. Rev. B* **62** R2283 (2000)
6. Müller M, Bleuse J, André R *Phys. Rev. B* **62** 16886 (2000)
7. Krizhanovskii D N et al. *Solid State Commun.* **118** 583 (2001)
8. Malpuech G et al. *Phys. Rev. B* **65** 153310 (2002)
9. Tartakovskii A I et al. *Phys. Rev. B* **67** 165302 (2003)
10. Stevenson R M et al. *Phys. Rev. Lett.* **85** 3680 (2000)
11. Tartakovskii A I, Krizhanovskii D N, Kulakovskii V D *Phys. Rev. B* **62** R13298 (2000)
12. Stevenson R M et al. *Phys. Rev. Lett.* **85** 3680 (2000)
13. Ciuti C et al. *Phys. Rev. B* **62** R4825 (2000); Ciuti C, Schwendimann P, Quattropani A *Phys. Rev. B* **63** 041303 (2001)
14. Baumberg J J et al. *Phys. Rev. B* **62** R16247 (2000)
15. Houdré R et al. *Phys. Rev. Lett.* **85** 2793 (2000)
16. Whittaker D M *Phys. Rev. B* **63** 193305 (2001)
17. Savvidis P G et al. *Phys. Rev. B* **64** 075311 (2001)
18. Saba M et al. *Nature* **414** 731 (2001)
19. Gippius N et al., in *Proc. of the 26th Intern. Conf. on the Physics of Semiconductors, Edinburgh, UK, 29 July – 2 August 2002* (Institute of Physics Conf. Ser., No. 171, Eds A R Long, J H Davies) (Bristol: IOP Publ., 2003) p. G4-6
20. Gippius N A et al. *Europhys. Lett.* **67** 997 (2004)
21. Gippius N A, Tikhodeev S G *J. Phys. C: Condens. Matter* **16** S3653 (2004)
22. Gippius N A et al. *Usp. Fiz. Nauk* **175** 327 (2005) [*Phys. Usp.* **48** 306 (2005)]
23. Whittaker D M, in *Proc. of PLCMN4, St. Petersburg, June 2004* (2004)
24. Baas A et al. *Phys. Rev. A* **69** 023809 (2004)
25. Carusotto I, Ciuti C *Phys. Rev. Lett.* **93** 166401 (2004)